

Accepted Manuscript

Crotoxin from *Crotalus durissus terrificus* venom: *In vitro* cytotoxic activity of a heterodimeric phospholipase A₂ on human cancer-derived cell lines

Silvana Pinotti Muller, Viviane Aline Oliveira Silva, Ana Vitória Pupo Silvestrini, Luana Henrique de Macedo, Guilherme Ferreira Caetano, Rui Manuel Reis, Mauricio Ventura Mazzi

PII: S0041-0101(18)30714-1

DOI: <https://doi.org/10.1016/j.toxicon.2018.10.306>

Reference: TOXCON 6003

To appear in: *Toxicon*

Received Date: 23 August 2018

Revised Date: 3 October 2018

Accepted Date: 29 October 2018

Please cite this article as: Muller, S.P., Silva, V.A.O., Silvestrini, Ana.Vitó.Pupo., de Macedo, L.H., Caetano, G.F., Reis, R.M., Mazzi, M.V., Crotoxin from *Crotalus durissus terrificus* venom: *In vitro* cytotoxic activity of a heterodimeric phospholipase A₂ on human cancer-derived cell lines, *Toxicon* (2018), doi: <https://doi.org/10.1016/j.toxicon.2018.10.306>.

This is a PDF file of an unedited manuscript that has been accepted for publication. As a service to our customers we are providing this early version of the manuscript. The manuscript will undergo copyediting, typesetting, and review of the resulting proof before it is published in its final form. Please note that during the production process errors may be discovered which could affect the content, and all legal disclaimers that apply to the journal pertain.



Crotoxin from *Crotalus durissus terrificus* venom: *in vitro* cytotoxic activity of a heterodimeric phospholipase A₂ on human cancer-derived cell lines

Silvana Pinotti Muller^{a,1}, Viviane Aline Oliveira Silva^{b,1}, Ana Vitória Pupo Silvestrini^c, Luana Henrique de Macedo^c, Guilherme Ferreira Caetano^a, Rui Manuel Reis^{b,d,e}, Mauricio Ventura Mazzi^{a*}

^aGraduate Program in Biomedical Sciences, Hermínio Ometto University Center, UNIARARAS, Av. Dr. Maximiliano Baruto 500, 13607-339, Araras, SP, Brazil.

^bMolecular Oncology Research Center, Barretos Cancer Hospital, Barretos, SP, Brazil;

^cSchool of Pharmaceutical Sciences of Ribeirão Preto, University of São Paulo-FCFRP-USP-Ribeirão Preto, SP, Brazil.

^dLife and Health Sciences Research Institute (ICVS), University of Minho, Braga, Portugal;

^eICVS/3B-PT Government Associate Laboratory, Braga, Portugal.

¹Contributed equally to this paper

*Correspondence to: M. V. Mazzi, Graduate Program in Biomedical Sciences, Hermínio Ometto University Center, UNIARARAS, Av. Dr. Maximiliano Baruto 500, 13607-339, Araras, SP, Brazil

Tel: 55-19-35431400

E-mail: maumazzi@fho.edu.br

Abstract

Crotoxin (CTX), a heterodimeric phospholipase present in venom of snakes of the genus *Crotalus*, has demonstrated a broad spectrum of pharmacological properties, such as antimicrobial, hemostatic, and antitumoral. However, the precise mechanism of its cytotoxicity and antitumoral properties remains to be determined. Therefore, in the present study, we isolated crotoxin (F1 CTX) through two steps DEAE-Sepharose and Heparin-Sepharose FF chromatography. The C-terminal sequence of the A- and B-chain protein fragment was determined by LC-MS/MS mass spectrometry, which showed 100% identity to crotoxin structure. In order to investigate its cytotoxic effects, we demonstrated that the F1 CTX fraction at 0 to 30 µg/mL concentrations for 72 h presented a heterogeneous response profile on nine human cancer-derived cell lines from four tumor types (pancreatic, esophagus, cervical cancer, and glioma). The glioma (GAMG and HCB151) and pancreatic (PSN-1 and PANC-1) cancer cells showed a higher sensitivity with IC₅₀ of <0.5, 4.1, 0.7 and <0.5 µg/mL, respectively. Conversely, F1 CTX does not reduce the viability of normal cells. On the other hand, cervical (SiHa) and esophagus (KYSE270) cancer cell lines presented higher resistance, with IC₅₀ higher than 30.2 and 8.7 µg/mL, respectively. Moreover, F1 CTX did not affect cell cycle distribution under the conditions evaluated and seems to be more cytotoxic than cytostatic. The pro-apoptotic effect of F1 CTX treatment was demonstrated in glioma (HCB151) cell line. In addition, crotoxin revealed a potential to initiate cell responses such as DNA damage in glioma (HCB151) and pancreatic cancer by H2AX activity induction. Conversely, F1 CTX does not reduce the viability of normal cells. Importantly, the comparison of F1 CTX effect with standard chemotherapeutic agents demonstrated a greater cytotoxic potential in the majority of tumor types (glioma, pancreatic, and cervical cancer). On the other hand, F1 CTX was less cytotoxic in esophageal cell lines compared to the gemcitabine agent used in clinical practice. Therefore, this work showed that F1 CTX has a cytotoxic activity and pro-apoptotic potential, contributing to the knowledge about the F1 crotoxin properties as well as its possible use in cancer research, particularly in glioma and pancreatic cancer cell lines.

28

Keywords: Crotoxin; snake venom; cytotoxicity; antitumor; glioma; pancreas

30

31

32 1. Introduction

33 Snakes of the genus *Crotalus* produce and secrete a complex of biologically active
34 substances, among them the phospholipase A₂ (PLA₂) (Calderon et al., 2014). Snake venom
35 PLA₂ (svPLA₂s) comprises a large class of molecules that catalyze the hydrolysis of sn-2
36 position phospholipids, releasing fatty acids and lysophospholipids. svPLA₂s are related to a
37 broad spectrum of biotechnological activities, including antitumoral, antimicrobial, and
38 hemostatic. The cytotoxic activity has been suggested to be a result of different cell death
39 mechanisms, which has been demonstrated *in vitro* in melanoma, neuroblastoma, and
40 leukemic cell lines (Baldi et al., 1998; Iglesias et al., 2005; Yan et al., 2007; Rodrigues et al.,
41 2009).

42 Among the PLA₂ isolated from snake venom, crotoxin (CTX), a β-neurotoxin, is a
43 heterodimeric complex composed of a toxic phospholipase (PLA₂) fraction, associated with
44 the non-enzymatic fraction crotapotin (Sobrinho et al., 2016). Parallel to its toxic effects,
45 numerous scientific findings have demonstrated the application of CTX in the pharmacological
46 field, with a broad spectrum of functional properties (Donato et al., 1996; Costa et al., 1997;
47 Sampaio et al., 2010). CTX cytotoxicity is mediated by specific interactions with cell surface
48 receptors and associated with transmembrane ligands, which are involved in cell damage
49 (Krizaj et al., 2000; Montecucco et al., 2008).

50 The antitumor and antiproliferative activity of CTX in different cancer cell lines including
51 leukemia, cervix, ovarian, lung, colon, renal, melanoma, and brain has been assessed in *in*
52 *vitro* and *in vivo* studies. According to these studies, the antiproliferative activity occurs
53 through apoptotic mechanisms, triggered by changes in mitochondrial membrane potential,
54 cytochrome C release, and caspase-3 activation (Corin et al., 1993; Newman et al., 1993;
55 Costa et al., 1998; Brigatte et al., 2016). CTX may also induce cell death by activation of
56 autophagy mechanisms, which was demonstrated in breast tumor cells (Yan et al., 2007).
57 Moreover, the ability of CTX to cause cytotoxic and memory antitumor immunity in mice have
58 been determined in lymphoma, adenocarcinoma, human lung squamous cell carcinoma and
59 esophageal cancer cell lines (Ferguson, Duncan, 2009; Wang et al., 2012; Qin et al., 2016).
60 Studies of CTX structure and function have brought relevant information for applications of
61 this molecule in the treatment of different types of cancer, including phase 1 clinical studies
62 for the treatment of refractory solid tumors associated with conventional therapies. CTX has

63 been investigated for its effective application in malignant tumor treatments, *in vivo* or *in vitro*,
64 alone or in combination with antitumor drugs (Rübsamen et al., 1971; Aird et al., 1989; Rudd
65 et al., 1994; Donato et al., 1996; Ye et al., 2011; Han et al., 2014; He et al., 2016). However,
66 new molecular mechanisms must be elucidated to apply the molecule in neoadjuvant
67 antitumor therapies.

68 To better understand the antitumor properties of CTX, in the present study, we isolated
69 crotoxin from *Crotalus durissus terrificus* snake venom, evaluated its response profile in nine
70 human cancer-derived cell lines, and analyzed its cytotoxicity, antiproliferative and pro-
71 apoptotic potential.

72

73 2. Materials and Methods

74 2.1. Reagents and venom

75 The yellowish *Crotalus durissus terrificus* venom was purchased from Koemitã Me
76 (Mococa, SP, Brazil). Sepharose G-75 and Heparin-Sepharose FF were purchased from
77 Amersham Life Science, Inc. All of the other reagents used in this study were of analytical
78 grade and purchased from Sigma Chem. Co, Merck and/or Synapse Biotechnology.

79

80 2.2. Purification of Crotoxin (CTX)

81 *C. durissus terrificus* crude venom (0.5 g) was applied to a DEAE-cellulose column,
82 which had previously been equilibrated with 0.05 M Tris-HCl, pH 7.5 (buffer A), and the
83 protein was eluted with 0.05 M Tris-HCl, pH 7.5 in a linear gradient of NaCl (0–1 M); 2 mL
84 fractions were collected. The eluted fraction with crotoxin activity was concentrated in an
85 ALPHA 2-4 LD plus Freeze-Dryer. Of the F4 CTX fraction, 50 mg were applied to the Heparin-
86 Sepharose FF column (HiTrap, heparin (HP), 5 mL), which had previously been equilibrated
87 with 0.01 M sodium phosphate, pH 7.0. The protein was eluted in linear gradient of NaCl (0–
88 1.5 M) at a flow rate of 2.5 mL/min, and 3 mL fractions were collected. The F1 CTX fraction
89 was pooled and functional and biochemical characteristics were assessed. Chromatography
90 was performed using the ÄKTAprime and liquid chromatography system (GE Healthcare).
91 Next, F1 CTX was subjected to identification and cytotoxic effects evaluation. All purification
92 and isolation procedures were performed at room temperature.

93

94 2.3. Identification of Crotoxin: internal peptide fragments

95 The purity of F1 CTX was determined by 15% (w/v) SDS-PAGE in a Tris-glycine buffer
96 of pH 8.3, for 120 min at 20 mA/100 V. The molecular mass was measured using the
97 Carestream Molecular Imaging Software (Carestream Health, Inc., 1994-2011) and at 10–260
98 kDa molecular weight calibration standards (Espectra™ Multicolor Broad Range).

99 The identification of crotoxin was determined by mass spectrometry. A coomassie
100 brilliant blue-stained crotoxin band (approximately 2 µg/spot) was cut out of the
101 polyacrylamide gel (13%) and digested “in-gel” for peptide mass fingerprinting and for internal

102 sequence determination. Five micrograms of isolated F1 CTX were reduced in 10 mM DTT,
103 alkylated in 50 mM of iodoacetamide, and then trypsinized in 20 ng/ μ L trypsin after gel
104 electrophoresis, according to the protocol reported by Shevchenko et al. (1996), with some
105 modifications. Tryptic fragments of the peptide were scored by the bond cleavage, and
106 charges on the C-terminus (a ions) and N-terminus (b ions) were generated. Peptide
107 identification was performed in a liquid chromatography-tandem mass spectrometer using a
108 C18 nanocolumn (LC-MS / MS Q-TOF PREMIER™). The resulting spectra were analyzed
109 using Mascot (Matrix Science) in the NCBI protein databases, with carbamidomethylation as
110 the fixed modification. The similarity between peptide sequences was assessed with BLAST.

111

112 2.4. Cytotoxic activity evaluation

113 2.4.1. Cell lines and cell culture

114 Nine immortalized human cancer-derived cell lines were used in the cytotoxicity
115 assays, comprising brain (glioma), pancreatic, cervical, and esophageal tumor models. In
116 addition, immortalized keratinocytes (hacat cells - ThermoFisher) and murine fibroblasts
117 (NIH/3T3 (ATCC® CRL-1658™) were used as non-cancer cells. Cells were cultivated in
118 Dulbecco's modified Eagle's medium (DMEM 1X, high glucose; Gibco, Invitrogen) or Le
119 Roswell Park Memorial Institute medium (RPMI-1640 1X, Gibco, Invitrogen) supplemented
120 with 10% fetal bovine serum (FBS) (Gibco, Invitrogen) and 1% penicillin/streptomycin solution
121 (Gibco, Invitrogen), at 37°C and 5% CO₂, as previously reported (Silva-Oliveira et al., 2016;
122 Silva et al., 2018). Authentication of cancer cell lines was conducted by the Diagnostic
123 Laboratory of Barretos Cancer Hospital (São Paulo, Brazil) as reported (Dirks et al., 2005;
124 Silva-Oliveira et al., 2016; Teixeira et al., 20016). The cell lines identities were confirmed by
125 genotyping, with the exception of U373, which was shown to be a subclone of the U251
126 lineage. In addition, a primary tumor culture (HCB151) was obtained from a glioblastoma
127 biopsy and provided by the Department of Neurosurgery of the Barretos Cancer Hospital
128 (Cruvinel-Carlioni et al., 2017).

129

130 2.4.2. Cell viability assay

131 The cytotoxic effect of F1 CTX or standard chemotherapeutic agents (paclitaxel (Sigma

132 - T7402), gemcitabine hydrochloride (Sigma - G6423), temozolomide (Sigma - T2577) and
133 cisplatin (Sigma - 479306) was analyzed by the MTS assay [3-(4,5-dimethylthiazol-2-yl)-5-(3-
134 carboxymethoxyphenyl)-2-(4-sulfophenyl)-2H-tetrazolium], (Cell Titer 96 Aqueous cell
135 proliferation assay-MTS, PROMEGA). Cell viability was determined by the survival rate, after
136 incubation with the MTS reagent (2h; 37°C, 5% CO₂) in the cell culture (until a maximum 5 x
137 10³ cells/well), which was treated with increasing concentrations of F1 CTX (0.5–30 µg/mL or
138 standard chemotherapeutic agents (0.5–150 µg/mL); 72h), and compared to the control group
139 (1% DMSO, final concentration). The absorbance was measured spectrophotometrically
140 ($\lambda_{490\text{nm}}$) in an automatic microplate reader system (Varioskan, Thermo). The results obtained
141 in the cell viability assay with the different concentrations of F1 CTX or standard
142 chemotherapeutic agents were converted to percent viability in relation to the control (1%
143 DMSO) \pm SD. All the assays were done in triplicate and repeated at least three times. The
144 half-maximal inhibitory concentration (IC₅₀) was calculated by non-linear regression analysis
145 using GraphPad PRISM 5.1 (GraphPad Software, La Jolla California USA), as previously
146 reported (Teixeira et al., 2016).

147

148 2.4.4. Effects of CTX on cell cycle and apoptosis

149 The effects of F1 CTX on cell cycle and apoptosis was evaluated in HCB 151 (drug-
150 sensitive) and SiHa (drug-resistant) cell lines (1×10⁶ cells/well) using a concentration
151 equivalent to IC₅₀ value of each cell line for 24 h. For cell cycle analysis, cells were examined
152 using PI stain to determine DNA content and analyzed using Cycle Test kit (BD Biosciences)
153 following the manufacturer's recommended protocol. Apoptosis assays were performed using
154 the Annexin V-FITC kit (BD Biosciences) according to the manufacturer's recommendations.
155 The distribution profile (G1, S, and G2/M) and the percentage of apoptotic cells were
156 characterized by flow cytometry using the BD FACSCanto II reagent kit (BD Biosciences) and
157 analyzed with BD FACSDiva software (BD Biosciences).

158

159 2.4.5. Molecular Analysis by Western Blot

160 In a direct immunoblot experiment, HCB151, PANC-1, and SiHa cell lines (1×10⁶
161 cells/well) were exposed to IC₅₀ concentration values of F1 CTX for 24h. Protein samples,

162 previously obtained by cell lysis, were separated and analyzed by SDS-PAGE and transferred
163 to a Hybond-C nitrocellulose membrane (Amersham Biosciences, Little Chalfont, UK) using a
164 mini turbo transfer system (Trans-Blot[®] BioRad) as reported (Plescia et al., 2005).
165 Membranes were blocked for 1h (5% milk powder in TBS/0.1% Tween (TBS-T; pH = 7.6) and
166 incubated overnight (4°C) with the primary antibodies (p-H2AX, p-AKT, AKT, p-P44/42
167 (MAPK- ERK1/2), p44/42, p21, and β -tubulin) diluted 1:1000 (Cell Signaling Technology). The
168 washed membranes were incubated with the secondary antibody and coupled to horseradish
169 peroxidase, 1:5000 (Cell Signaling Technology). β -tubulin was used as loading control.
170 Protein bands were determined by chemiluminescence (ECL Western Blot Detection
171 Reagents, RPN2109, GE Healthcare) and signal intensity was assessed with the
172 ImageQuant[™] LAS 4000 mini photographic documentation system (GE Healthcare). The
173 densitometry analysis of immunoblots was performed with the Image J software (version 1.41;
174 National Institutes of Health).

175

176 5. Statistical analysis

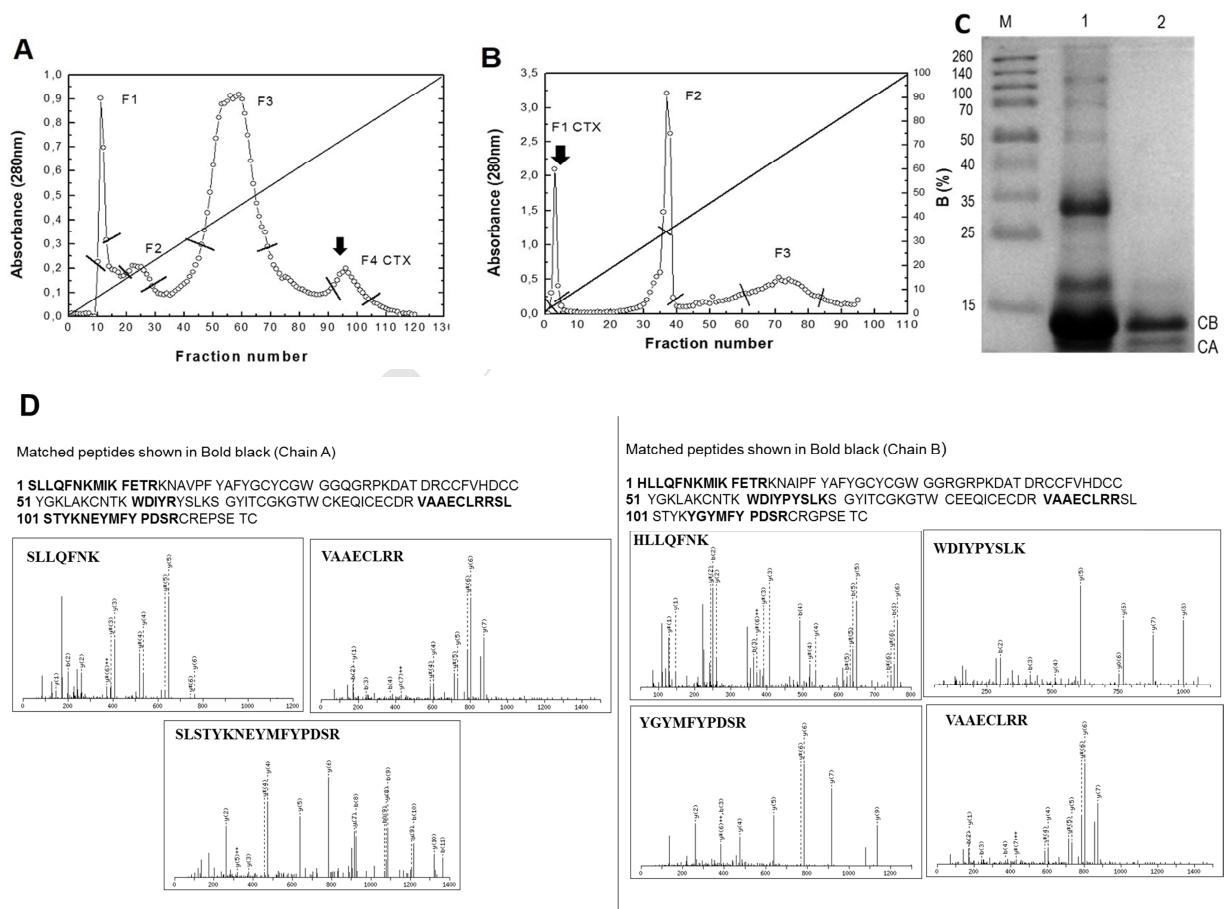
177 Student's t-test was used to compare each experimental group with the control group.
178 The p value <0.05 indicated a significant difference between the samples. Graphs and
179 statistical analysis were performed in GraphPad Prism 5.1 software.

180

181 **3. Results**182 **3.1. Purification and identification of CTX**

183 The F1 CTX molecule was isolated in two chromatographic steps: first, by exclusion
 184 chromatography using a DEAE-cellulose column (Figure 1A), and second, by bioaffinity
 185 chromatography in a Heparin-Sepharose FF column (Figure 1B). The degree of purity was
 186 assessed by SDS-PAGE revealing a dimeric, low molecular weight protein consisting of two
 187 subunits with apparent molecular weight between 14–15 kDa (Figure 1C). Further peptide
 188 fragments identified in the mass fingerprinting corresponding to MS/MS fragmentation of three
 189 internal peptide fragments (Chain A) and four fragments (Chain B), confirmed the molecular
 190 identity of crotoxin (Figure 1D).

191

Fig. 1

192

193

194 3.2. CTX cytotoxic profile

195 CTX cytotoxic potential was determined by MTS assays in brain (glioma), pancreatic,
196 cervical, and esophageal cancer cells at different concentrations (0 to 30 $\mu\text{g}/\text{mL}$). The authors
197 suggested F1 CTX might be a selective anti-cancer agent, discriminating between normal and
198 tumor cells. The dose-response curves showed that cell lines exhibited a heterogeneous
199 cytotoxic profile in response to F1 CTX (Figure 2 and table 1). The mean IC_{50} was 8.6 $\mu\text{g}/\text{mL}$
200 and varied significantly between cell lines, with differences of more than sixty-fold (IC_{50} range:
201 $<0.5 - >30 \mu\text{g}/\text{mL}$) (Table 1). The KYSE 30 (esophageal), GAMG, HCB151 (glioma), PSN-1,
202 PANC-1 (pancreatic), and HeLa (cervical) tumor cells showed higher sensitivity, with IC_{50} of
203 1.0, <0.5 , 4.1, 0.7, <0.5 , and 2.4 $\mu\text{g}/\text{mL}$, respectively (Figure 2 A, C, E, F, G and H). On the
204 other hand, the KYSE 270 (esophageal), U373 (glioma), and SiHa (cervical) cells exhibited
205 higher resistance, with IC_{50} of 8.7, 30.2 and $>30.0 \mu\text{g}/\text{mL}$, respectively (Figure 2 B, D, and I).
206 In contrast, identical concentrations of F1 CTX did not reduce the viability of normal human
207 keratinocytes (HaCaT) or mouse fibroblasts (3T3) cell lines on the same conditions of assay
208 (Figure 2 J and K).

209 Additionally, we compared the F1 CTX cytotoxic potential with standard
210 chemotherapeutic agents for glioma, pancreatic, esophagus, and cervical cancer. CTX
211 treatment was more cytotoxic in the majority of tumor types (glioma, pancreatic, and cervical
212 cancer). In contrast, F1 CTX was less cytotoxic in esophageal cell lines compared to the
213 gemcitabine agent used in clinical practice (Table 1).

214

215

216

217

218

219

220

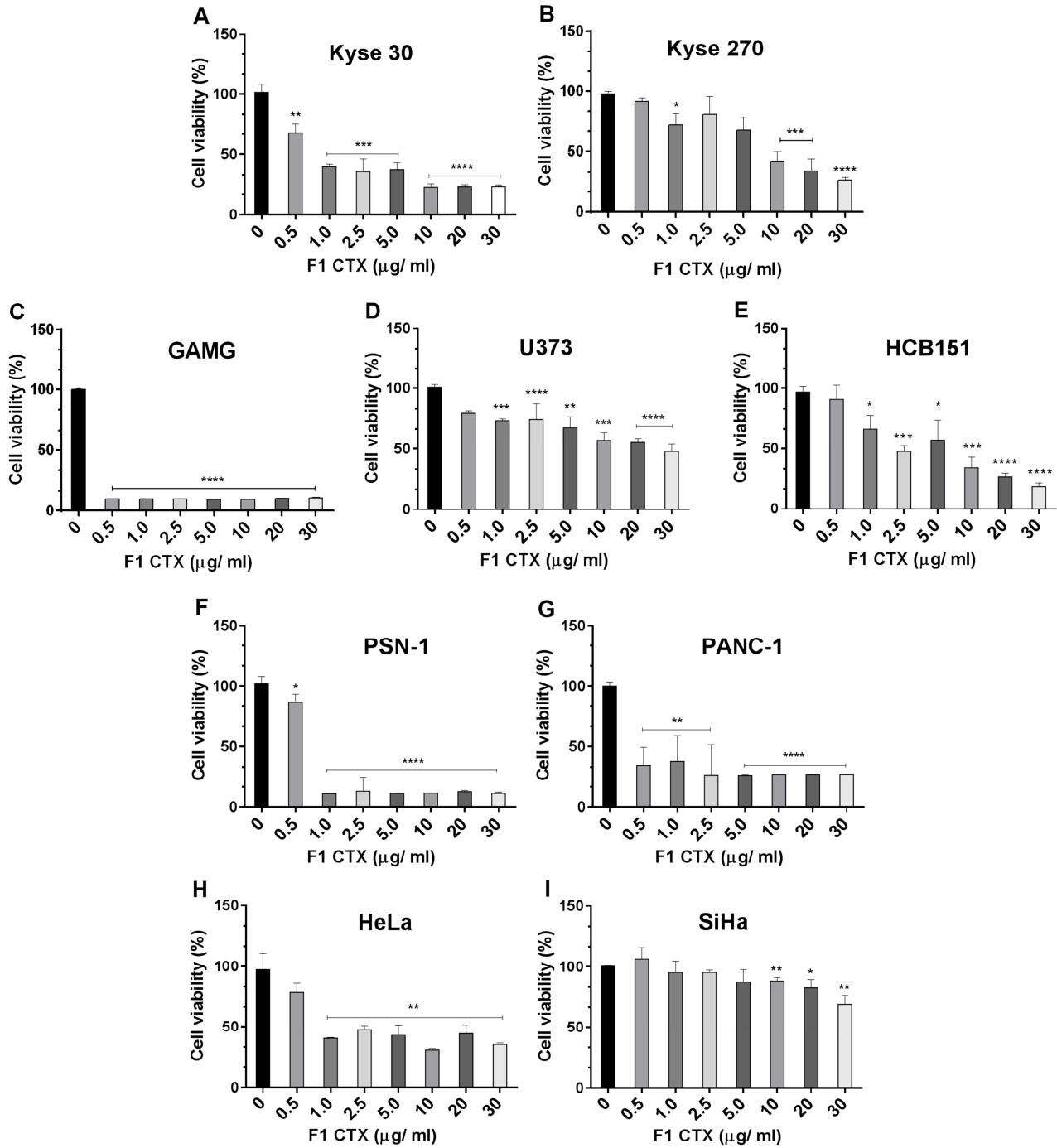
221

222

223

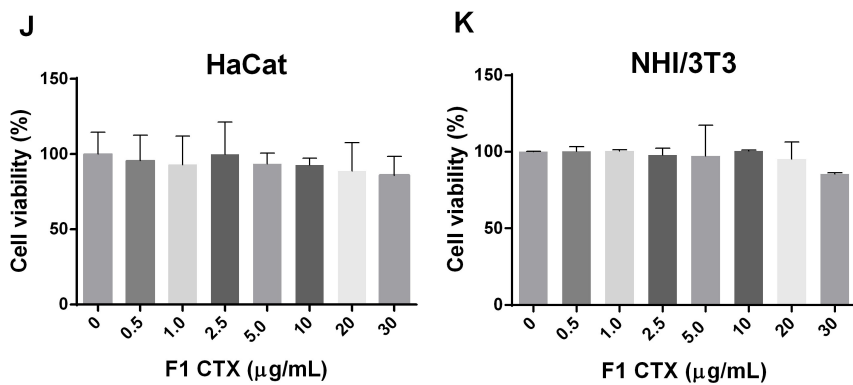
Fig. 2

224



225

226
227
228
229
230
231
232
233



234
235
236
237
238
239
240
241
242
243
244
245
246
247
248
249
250
251
252
253
254
255
256
257
258

259 **3.3. CTX antiproliferative and pro-apoptotic effects**

260 Since we observed a cytotoxic effect of F1 CTX in cancer cells, we further determined
261 its effect on cell cycle distribution and cell death using flow cytometric analysis. As shown in
262 Figure 3 (A,B,C,D), no significant effect was observed in drug-sensitive (HCB151 – 4.1 μ g/mL)
263 or drug-resistant cells (SiHa -30 μ g/mL) after toxin treatment, suggesting that CTX at
264 concentrations used has no interference on cell cycle distribution under the conditions
265 evaluated (Figure 3 B,D). Next, we examined the apoptosis-inducing effect of F1 CTX. The
266 basal population of early and late apoptotic cells in the untreated cultures was 0.6% and 0.1%
267 (HCB 151) and 4.8% and 7.2% (SiHa). However, when cancer cells were treated with F1 CTX
268 at IC₅₀ value for 24 h, the apoptotic cells (early + late apoptosis) increased by 13.2% and
269 11.0% (HCB 151) compared to the control cells (Figure 4 A,B). No significant effect was
270 observed in SiHa cell (Figure 4 C,D).

271

272

273

274

275

276

277

278

279

280

281

282

283

284

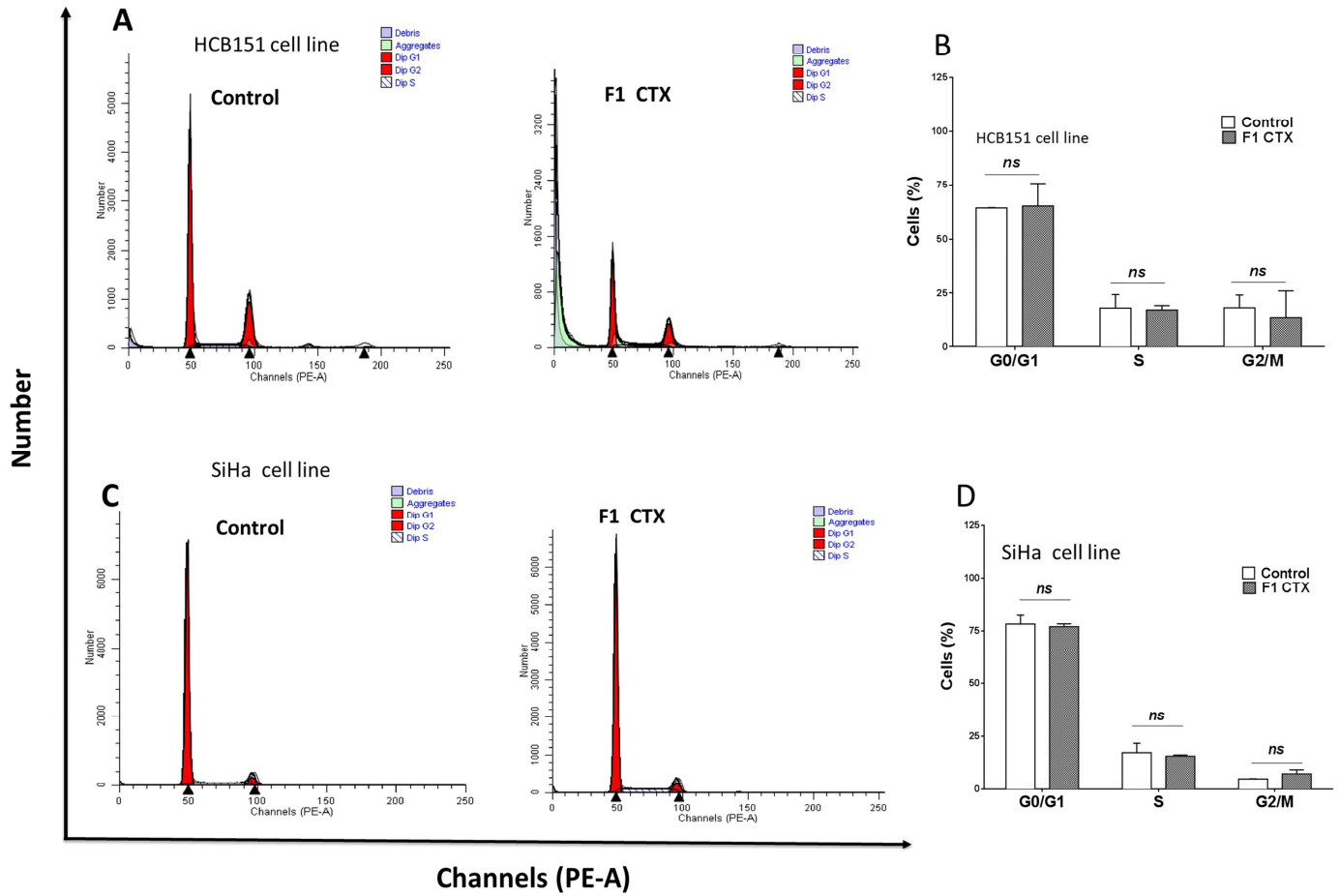
285

286

287

288

Fig. 3



289

290

291

292

293

294

295

296

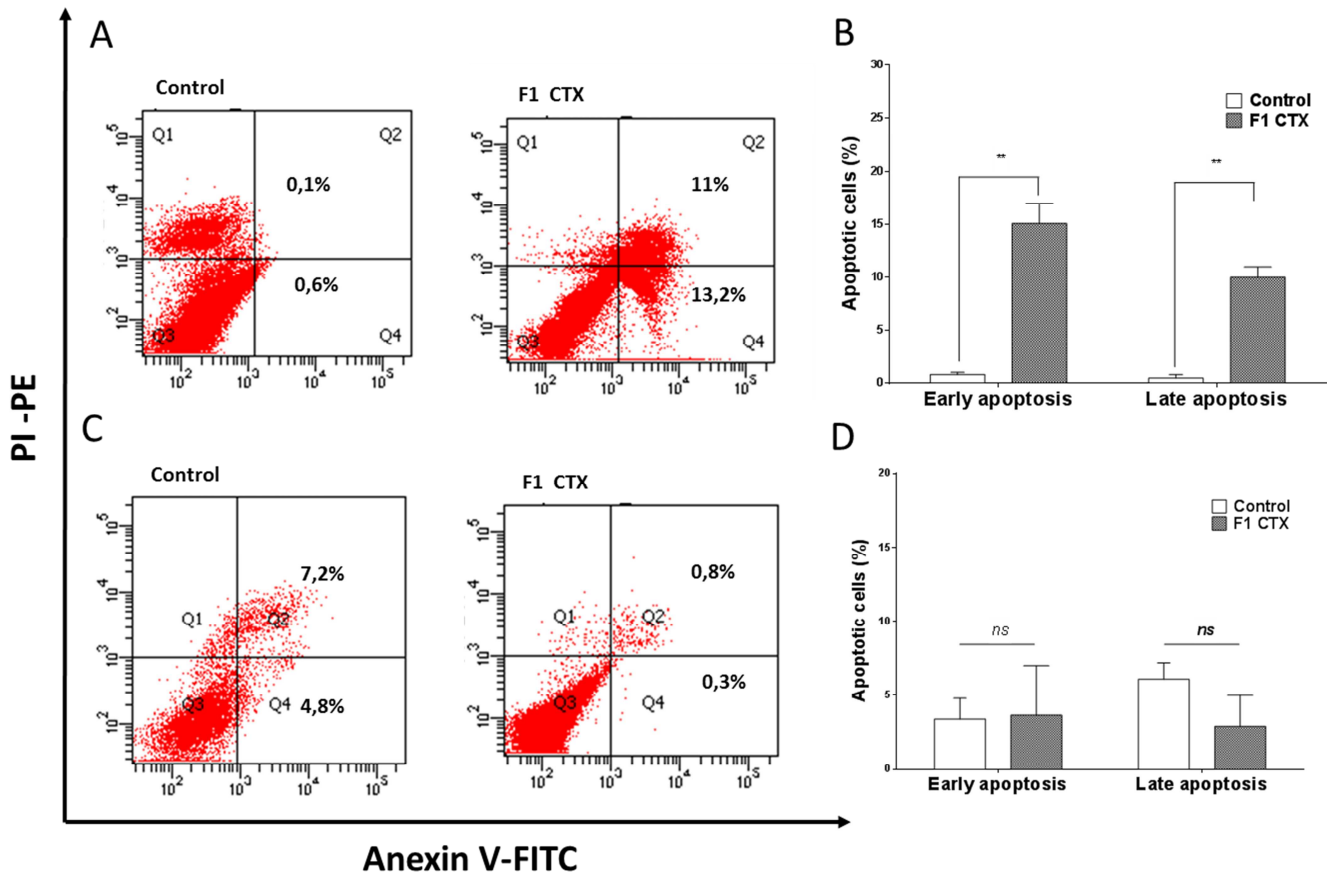
297

298

299

300

Fig. 4



301

302

3.4. Effects of CTX on cell signaling

303

304

305

306

307

308

309

To better explore the underlying mechanisms of F1 CTX, we assessed the expression of the main proteins related to proliferation/survival and DNA damage mechanism induced by molecule. The protein expressions after F1 CTX treatment in cancer cells (HCB151, PANC-1 and SiHa) were quantified relative to untreated control cells. As shown in Figure 5, we observed an increase of H2AX phosphorylation, an important marker of DNA damage in HCB151 cells; it was remarkably upregulated in PANC-1 (Figure 5 A, B). p21 expression, an important cell cycle regulator, did not change in any cell lines corroborating the data obtained

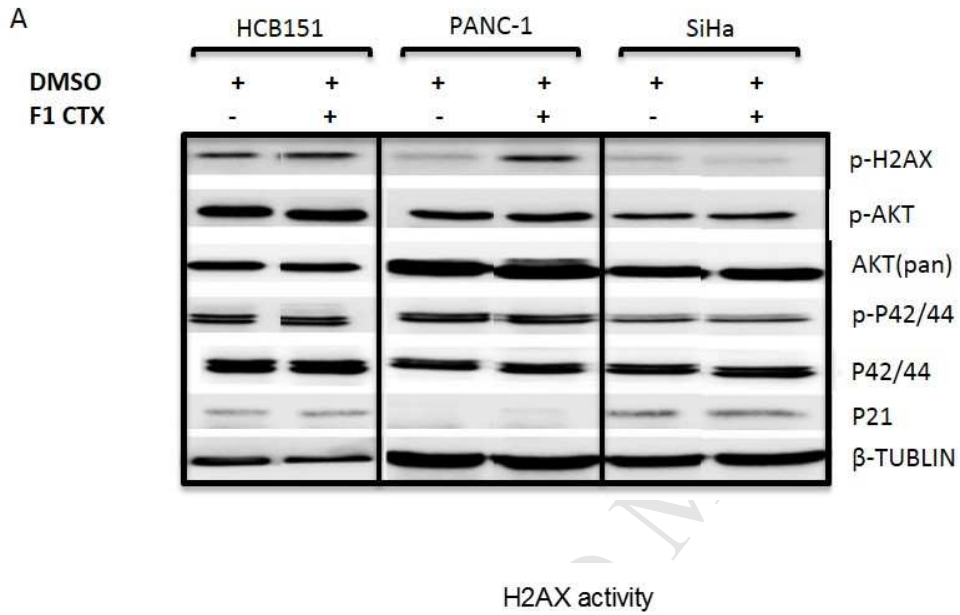
310 through flow cytometry. In addition, no change in response to CTX was observed for p-AKT,
 311 AKT (pan), pP42/44 and P42/44 in the three cell lines evaluated (Figure 5 A)

312

313

314

Fig. 5



315

316

317

318

319

320

321

322

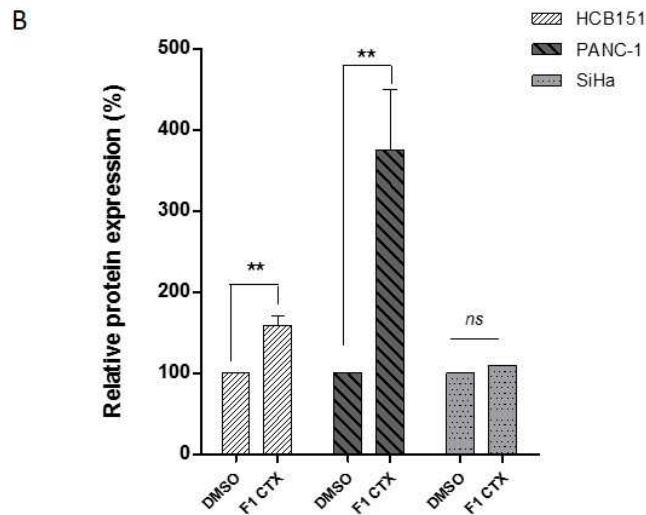
323

324

325

326

327



328

329 **4. Discussion**

330 In this study, crotoxin, a phospholipase A2 from *Crotalus durissus terrificus* venom was
331 purified to homogeneity in a two-step procedure using ion exchange chromatography followed
332 Heparin Sepharose affinity chromatographic. Due to its unique structure and surface charge
333 distribution, the heparin matrix was able to interact strongly with some components in the
334 crude venom, whereas crotoxin (F1 CTX) showed a low affinity to the column (Figure 1).
335 Crotoxin is a heterodimeric complex consisting of a weakly basic, toxic, and non-hemolytic
336 PLA₂ (B subunit or crotoxin CB) and an acid, non-toxic, non-enzymatic and hemolytic
337 component known as crotopotin (A subunit or crotoxin CA) that potentiates the toxicity of the
338 molecule, acting as a chaperone protein (Neumann, Habermann, 1955; Fraenkel-Conrat,
339 Singer, 1956; Fraenkel-Conrat, 1971; Marlas, Bon, 1982; Radvanyl, Bon, 1982; Andrião-
340 Escarso et al., 2002; Faure, Saul, 2012). The subunit CB or PLA₂ presents about 14 kDa,
341 isoelectric point 9.7, consisting of a single polypeptide chain of 122 amino acid residues,
342 stabilized by seven disulfide bridges (Aird et al., 1989; Faure, Saul, 2012). The CA subunit
343 (crotopotin) has a molecular weight of 8.9 kDa, isoelectric point of 3.4, and has no enzymatic
344 or toxic activities (Rübsamen et al., 1971; Bon et al., 1989). Faure et al., (2012) have been
345 demonstrated that this subunit comprises three covalently linked polypeptide chains (α , 39
346 residues, β , 35 residues and γ , 14 residues). Our results showed peptide fragments that were
347 generated by mass fingerprinting and confirmed the identity of both A and B subunits of
348 crotoxin (Figure 1). Some authors suggest that combinations of these subunit complexes or
349 post-translational modifications originate the different described isoforms of CTX (Faure et al.,
350 1988; Faure et al., 1991; Faure et al., 1993).

351 We first investigated the cytotoxic profile of F1 CTX action against four different types
352 of solid tumor cell lines. In our studies, the lowest IC₅₀ value (>0.5 μ g/mL) was found for the
353 pancreatic tumor cell line (PANC-1) and glioma (GAMG), which demonstrated greater
354 sensitivity. Notably, F1 CTX also promoted cytotoxicity in HCB151, PSN-1, PANC-1, HeLa,
355 and KYSE 30 cell lines. In contrast, purified CTX exerted significantly lower cytotoxicity in the
356 esophageal tumor cell line (KYSE 270), presenting an IC₅₀=8.7 μ g/mL. In the same way, we
357 observed a greater resistance for glioma (U373, IC₅₀=30.1 μ g/mL) and cervical cancer (SiHa,
358 IC₅₀>30 μ g/mL) cells. Our study was performed in according to the criterion adopted by

359 American National Cancer Institute (NCI) to consider an extract promising for preclinical
360 studies when IC₅₀ values presented are lower than 30 µg/mL for 72 h (<http://www.cancer.gov>)
361 (Chou, Talalay, 1984; Suffness, Pezzuto, 1990; Talib, Mahasneh, 2010; Kuete et al., 2013;
362 Trendowski, 2015).

363 Thus, our results demonstrated that the isolated CTX presented cytotoxic effects on
364 different tumor cell lines with a heterogeneous response profile. One of the main objectives of
365 targeted cancer therapy is to selectively eliminate tumor cells while sparing normal tissues.
366 Although, we had no normal counterpart available for many of the tissues evaluated, we used
367 mouse fibroblasts and human normal keratinocytes, which are strongly affected by anti-
368 neoplastic chemotherapies (Plescia et al., 2005) to compare cytotoxic potential of CTX. We
369 demonstrated that CTX had no effect on viability of normal human keratinocytes (HaCaT) or
370 mouse fibroblasts (3T3) cell lines at concentrations tested. Ferguson and Duncan (2009)
371 reported significant cytotoxic activity with *Crotalus durissus terrificus* PLA₂ on colon
372 adenocarcinoma (HT29), melanoma (B16F10), and breast adenocarcinoma (MCF-7) cells
373 with an IC₅₀ of 40, 108.3, and 308.6 µg/mL respectively. In order to reduce the toxicity of the
374 molecule, these authors conjugated PLA₂ with dextrin by the polymer masked-unmasked
375 protein therapy method and showed that the conjugate presented a marked reduction in
376 hemolytic activity and greater cellular cytotoxicity, but with an IC₅₀ value of 16.3 µg/mL for
377 HT29, and 62.9 µg/mL for MCF-7. In a previous study, Rudd et al. (1994) highlighted that
378 crotoxin displays low toxicity in normal cells, suggesting its selective toxicity to tumors.

379 The ant proliferative and cytotoxic activities of CTX have been demonstrated through
380 cell cycle arrest and pro-apoptotic mechanisms (Costa et al., 1998; Ferguson, Duncan, 2009;
381 Wang et al., 2012; Han et al., 2014). However, we did not observe interference on cell cycle
382 distribution under the conditions evaluated. This finding seems to be in disagreement with
383 studies with lung adenocarcinoma (A-549), esophagus (ECA-109), and lung carcinoma (SK-
384 MES-1) lines (Rudd et al., 1994; He et al, 2013; Han et al., 2014), which demonstrated growth
385 inhibitory effects by cell cycle arrest. To further explore the role of CTX in cell death
386 mechanism, we investigated its effect in protein expression related to DNA damage,
387 proliferation/survival and cell death. The pancreatic (PANC-1) cell line exhibited a significant
388 upregulation of H2AX activity, suggesting possible DNA damage effect (Ivashkevich et al.,
389 2012; Siddiqui et al., 2015; Ji et al., 2017). Likewise, the glioma cell line (HCB 151) showed a

390 slight increase of H2AX activity and increased percentage of apoptotic cells (early + late
391 apoptosis) after CTX treatment evaluated by flow cytometer. Therefore, CTX exposure
392 induced alterations in different pathways involved in DNA damage and mortality. Studies have
393 shown that the molecular cytotoxic mechanisms of PLA₂ involve the regulation of different
394 signaling pathways, and that this effect is dependent of enzymatic activity. These studies
395 revealed that the dissociation of the complex and the enzymatic activity are necessary for
396 cytotoxicity, because when the catalytic activity of the complex or the PLA₂ subunit is
397 alkylated, cytotoxic activity is lost (Corin et al., 1993; Soares, Giglio, 2003; Marchi-Salvador et
398 al., 2008; Sobrinho et al., 2016).

399 The pro-apoptotic effect of CTX has been shown to trigger changes in mitochondrial
400 membrane potential, cytochrome C release, and caspase-3 activation (Donato et al., 1996;
401 Costa et al., 1997; Sampaio et al., 2010; Sobrinho et al., 2016). It has also been
402 demonstrated that CTX induces cell death by autophagy mechanisms in breast and lung
403 cancer cells (Yan et al., 2007; Han et al., 2014) and inhibits the growth of Eca-109 cells *in*
404 *vitro* via apoptosis induction and G1 phase arrest (Ye et al., 2011). Interestingly, Wang et al
405 (2012) showed that the combination of CTX with tyrosine kinase inhibitor gefitinib (Iressa[®])
406 significantly enhanced the antitumor activity of gefitinib and caused increased damage to
407 blood vessels and reduced tumor size *in vivo*. These studies suggest that CTX cell
408 cytotoxicity depends on tumor type, which may indicate distinct mechanisms of action.

409 In addition, we compared the effect of CTX with standard chemotherapeutic agents for
410 glioma, pancreatic, esophagus, and cervical cancer. Our results demonstrated that crotoxin
411 treatment was more cytotoxic than their corresponding chemotherapeutics in the majority of
412 tumor types (glioma, pancreatic, and cervical cancer). Once the synergy (chemo-
413 sensitization) of known and new compounds are of major interest, this study opens new
414 perspectives for classical chemotherapy. However, the response level seen in practice is still
415 suboptimal and there is an urgent need for improvement (Wiedmann, Mossner, 2013;
416 Voutsadakis, 2011). Our results provide insights for further studies with CTX as an interesting
417 antineoplastic agent in glioma and pancreas cancer lines.

418

419 5. Conclusions

420 In conclusion, F1 CTX fraction from *Crotalus durissus terrificus* was purified with

421 electrophoretic homogeneity. Purified hetero-dimer enzymes showed significant cytotoxicity
422 exhibiting substantial activity against several cancer cell lines, while normal cell lines were
423 not affected. Mechanistically, F1 CTX promotes pro-apoptotic effects and induces a potential
424 DNA damage on pancreatic (PANC-1) and glioma (HCB151) cell lines, revealed through the
425 increase in H2AX activity. Interestingly, F1 CTX demonstrated a greater cytotoxic potential
426 than the specific standard chemotherapeutic agents used in clinical practice in the majority of
427 tumor types (glioma, pancreatic, and cervical cancer). These results add to the functional
428 knowledge database on crotoxin, and provide new insights into the development of antitumor
429 therapy.

430

431 **Acknowledgments**

432 The current study was supported by grants from FAPESP, the Hermínio Ometto University
433 Center, the Hospital de Cancer de Barretos and FINEP (MCTI/FINEP/MS/SCTIE/DECIT-
434 01/2013 - FPXII-BIOPLAT). We acknowledge the Mass Spectrometry Laboratory of the
435 Brazilian Biosciences National Laboratory, CNPEM, Campinas, Brazil, for providing support
436 on mass spectrometry analysis.

437

438 **Ethical statement**

439 The experiments followed the methodology recommended by the international ethical
440 standards of the scientific committee of our university (process nº 847/2015).

441

442

443 **References**

- 444 Aird, S.D., Steadman, B.L., Middaugh, C.R., Kaiser, I.I., 1989. Comparative spectroscopic
445 studies of four crotoxin homologs and their subunits. *Biochim. Biophys. Acta.* 31, 211–
446 218. DOI: [10.1016/0167-4838\(89\)90189-1](https://doi.org/10.1016/0167-4838(89)90189-1).
- 447
448 Andrião-Escarso, S. H., Soares, A. M., Fontes, M. R., Fuly, A. L., Correa, F. M., Rosa, J.
449 C., Greene, L. J., Giglio, J. R., 2002. Structural and functional characterization of an acidic
450 platelet aggregation inhibitor and hypotensive phospholipase A2 from *Bothrops*
451 *jararacacussu* snake venom. *Biochem Pharmacol.* 64, 723-732. DOI:[10.1016/s0006-](https://doi.org/10.1016/s0006-2952(02)01210-8)
452 [2952\(02\)01210-8](https://doi.org/10.1016/s0006-2952(02)01210-8)
- 453
454 Baldi, A., Mordoh, J., Medrano, E.E. Medrano, Bonaparte, Y.P., Lustig, E.S., Rumi, L.,
455 1998. Special report: studies to determine the possible antitumoral properties of cobra
456 venom and crotoxin complex A and B. *Medicina.* 48, 337-344.
- 457
458 Bon, C., Bouchier, C., Choumet, V., Faure, G., Jiang, M.S., Lambezat, M.P., Radvanyi, F.,
459 Saliou, B., 1989. Crotoxin, half-century of investigations on a phospholipase A2
460 neurotoxin. *Acta Physiol. Pharmacol. Latin. Am.* 39, 439–448.
- 461
462 Brigatte P., Faiad, O.J., Ferreira Nocelli, R.C., Landgraf, R.G., Palma, M.S., Cury, Y. Cury,
463 R., Sampaio, S.C., 2016. Walker 256 Tumor Growth Suppression by Crotoxin Involves
464 Formyl Peptide Receptors and Lipoxin A₄. *Mediators Inflamm.* 2016, 1-11. DOI:
465 [10.1155/2016/2457532](https://doi.org/10.1155/2016/2457532).
- 466
467 Calderon, L.A., Sobrinho, J.C., Zaqueo, K.D., de Moura, A.A., Grabner, A.N., Mazzi, M.V.,
468 Marcussi, S., Nomizo, A., Fernandes, C.F.C., Zuliani, J.P., Carvalho, B.M.A., S.L. da Silva,
469 Stábeli, R.G., Soares, A.M., 2014. Antitumoral Activity of Snake Venom Proteins: New
470 Trends in Cancer Therapy. *BioMed Res. Int.* 2014, 1-19. DOI: [10.1155/2014/203639](https://doi.org/10.1155/2014/203639).
- 471
472 Chou, T.-C., Talalay, P., 1984. Quantitative analysis of dose-effect relationships: the
473 combined effects of multiple drugs or enzyme inhibitors *Adv. Enzyme Regul.*, 22, 27–55.
474 DOI:[10.1016/0065-2571\(84\)90007-4](https://doi.org/10.1016/0065-2571(84)90007-4).
- 475
476 Corin, R.E., Viskatis, L.J., Vidal, J.C., Etcheverry, M.A., 1993. Cytotoxicity of crotoxin on
477 murine erythroleukemia cells in vitro. *Invest. New Drugs.* 11, 11-15.
- 478
479 Costa, L.A., Miles, H., Araujo, C.E., Gonzalez, S., Villarrubia, V.G., 1998. Tumor
480 regression of advanced carcinomas following intra and or peri-tumoral inoculation with
481 vrctc-310 in humans: preliminary report of two cases. *Immunopharmacology and*
482 *immunotoxicology.* 20, 15-25. DOI:[10.3109/08923979809034806](https://doi.org/10.3109/08923979809034806).
- 483
484 Costa, L.A., Miles, H.A., Diez, R.A., Araujo, C.E., Coni, M.C.M., Cervellino, J.C., 1997.
485 Phase I study of VRCTC-310, a purified phospholipase A2 purified from snake venom, in
486 patients with refractory cancer: safety and pharmacokinetic data. *Anticancer dRUGs.* 9,
487 829-834. DOI: [10.1097/00001813-199710000-00003](https://doi.org/10.1097/00001813-199710000-00003).
- 488
489 Cruvinel-Carlioni, A., Silva-Oliveira, R., Torrieri, R., Bidinotto, L.T., Berardinelli, G.N. B,

- 490 Oliveira-Silva, V.A., Clara, C.A., de Almeida, G.C., Martinho, O., Squire, J.A., Reis, R.M.,
491 2017. Establishment and Molecular Characterization of Short-term Glioblastoma Primary
492 Cultures. *Translational Cancer Research*. 6, 332-345. DOI: 10.21037/tcr.2017.03.32.
493
- 494 Dirks, W.G., Faehnrich, S., Estella, I.A., Drexler, H.G., 2005. Short tandem repeat DNA
495 typing provides an international reference standard for authentication of human cell lines.
496 *Altex*. 22, 103-109.
497
- 498 Donato, N.J., Martin, C.A., Perez, M., Newman, R.A., Vidal, J.C., Etcheverry, M. E., 1996.
499 Regulation of epidermal growth factor receptor activity by crotoxin, a snake venom
500 phospholipase A2 toxin. A novel growth inhibitory mechanism. *Biochem. Pharmacol.* 11,
501 1535–1543. DOI: 10.1016/0006-2952(96)00097-4.
502
- 503 Faure, G., Bon, C., 1988. Crotoxin, a phospholipase A₂ neurotoxin from the South
504 American rattlesnake, *Crotalus durissus terrificus*: purification of several isoforms and
505 comparison of their molecular structure and of their biological
506 activities. *Biochemistry*, 27, 730–738.
507
- 508 Faure, G., Guillaume, J.-L., Camoin, L., Saliou, B., Bon, C., 1991. Multiplicity of acidic
509 subunit isoforms of crotoxin, the phospholipase A₂ neurotoxin from *Crotalus durissus*
510 *terrificus* venom, results from posttranslational modifications. *Biochemistry*, 30, 8074–
511 8083.
512
- 513 Faure, G., Harvey, A.L., Thomson, E., Saliou, B., Radvanyi, F. Bon, C., 1993.
514 Comparison of crotoxin isoforms reveals that stability of the complex plays a major role
515 in its pharmacological action. *Eur. J. Biochim.*, 214, 491-496.
516
- 517 Faure, G. Saul, F., 2012. Crystallographic characterization of functional sites of crotoxin
518 and ammodytoxin, potent b-neurotoxins from Viperidae venom. *Toxicon*, 60, 531-538. DOI:
519 10.1016/j.toxicon.2012.05.009.
520
- 521 Ferguson, E.L., Duncan, R., 2009. Dextrin-phospholipase A2: synthesis and evaluation as
522 a bioresponsive anticancer conjugate. *Biomacromolecules*. 10, 358-1364.
523 DOI:10.1021/bm8013022.
524
- 525 Fraenkel-Conrat, H., Singer B., 1956. Fractionation and composition of crotoxin. *Arch*
526 *Biochem Biophys*. 60, 64-73.
527
- 528 Fraenkel-Conrat, R. A., 1971. Biological roles of the two components of crotoxin, *Proc.*
529 *Natl. Acad. Sci.* 68,1560-1563.
530
- 531 Han, R., Lian, H., Qin, Z., Liu, C., 2014. Crotoxin induces apoptosis and autophagy in
532 human lung carcinoma cells in vitro via activation of the p38 MAPK signaling pathway.
533 *Acta Pharmacologica Sin.* 35, 1323-1332. DOI: 10.1038/aps.2014.62.
534
- 535 He, J.K., Wu, X., Wang, Y., Han, R., Qin, Z., Xie, Y., 2013. Growth inhibitory effects and
536 molecular mechanisms of crotoxin treatment in esophageal Eca-109 cells and transplanted
537 tumors in nude mice. *Acta Pharmacologica Sin.* 34, 295–300. DOI:10.1038/aps.2012.156.

- 538
539 Iglesias, C.V., Aparicio, R., Rodrigues-Simioni, L., Camargo, E.A., Antunes E., Marangoni,
540 S. Marangoni, Toyama, D. de O., Beriam, L.O.S., Monteiro, H.S.A., Toyama, M.H., 2005.
541 Effects of morin on snake venom phospholipase A2 (PLA2). *Toxicon*. 46, 751-758. DOI:
542 10.1016/j.toxicon.2005.07.017.
543
- 544 Ivashkevich, A., Redon, C. E., Asako, N. J., Martin, R. F., Martin, O. A., 2012. Use of the γ -
545 H2AX assay to monitor DNA damage and repair in translational cancer research. *Cancer*
546 *Letters*. 327,123-133. DOI: 10.1016/j.canlet.2011.12.025.
547
- 548 Ji, J., Zhang, Y., Redon, C. E., Reinhold, W.C., Chen, A. P., Fogli, L. K., Holbeck, S. L.,
549 Parchment, R. E., Hollingshead, M., Tomaszewski, J. E., Dudon, Q., Pommier, Y.,
550 Doroshow, J. H., Bonner, W. M., 2017. Phosphorylated fraction of H2AX as a
551 measurement for DNA damage in cancer cells and potential applications of a novel assay.
552 *Plos One*. 12, 1-18. DOI: 10.1371/journal.pone.0171582.
553
- 554 Krizaj, I., Gubensek, F., 2000. Neuronal receptors for phospholipases A2 and b-
555 neurotoxicity. *Biochimie*. 82, 807–814. DOI: 10.1016/S0300-9084(00)01172-X.
556
- 557 Kuete, V., Seo, E.-J., Krusche, B., Oswald, M., Wiench, B., Schröder, S., Efferth, T., 2013.
558 Cytotoxicity and pharmacogenomics of medicinal plants from traditional korean medicine.
559 *Evid Based Complement Alternat Med*. 2013, 1–14. DOI:10.1155/2013/341724.
560
- 561 Marchi-Salvador, D.P., Corrêa, L.C., Magro, A.J., Oliveira, C. Z., Soares, A. M., Fontes,
562 M.R. M., 2008. Insights into the role of oligomeric state on the biological activities of
563 crotoxin: crystal structure of a tetrameric phospholipase A2 formed by two isoforms of
564 crotoxin B from *Crotalus durissus terrificus* venom. *Proteins*, 72, 883-891, 2008.
565 DOI:10.1002/prot.21980
566
- 567 Marlas, G., Bon, C., 1982. Relationship between the pharmacological action of crotoxin
568 and its phospholipase activity, *Eur. J. Biochem*. 125,157-165.
569
- 570 Montecucco, C., Gutierrez, J.M., Lomonte, B., 2008. Cellular pathology induced by snake
571 venom phospholipase A2 myotoxins and neurotoxins: common aspects of their
572 mechanisms of action. *Cell. Mol. Life Sci*. 65, 2897–2912. DOI: 10.1007/s00018-008-
573 8113-3.
574
- 575 Neumann, W. P., Habermann, E., 1955. Crotoxin, the main toxin from venom from the
576 Brazilian rattlesnake, *Crotalus terrificus terrificus*. *Biochem*. 327,170-185.
577
- 578 Newman R.A., Vidal J.C., Viskatis, L.J., Johnson, J., Etcheverry, M.A., 1993. VRCTC-310,
579 a novel compound of purified animal toxin separates antitumor efficacy from neurotoxicity.
580 *Invest. New Drugs*. 11,151–159.
581
- 582 Plescia, J.anet, Salz, W., Xia, F., Pennati, M., Zaffaroni, N., Daidone, M. G., Meli, M. T. D.,
583 Fortugno, P., Nefedova, Y., Gabrilovich, D. I., Colombo, G., Altieri, D.C., 2005. Rational
584 design of shepherdin, a novel anticancer agent. *Cancer Cell*, 7, 457-468. DOI:
585 10.1016/j.ccr.2005.03.035.

- 586
587 Qin, H., Cha, S.S., Neelapu, S.S., Lou, Y., Wei, J., Liu, Y. J., Kwak, L.W., 2016. Vaccine
588 site inflammation potentiates idiotype DNA vaccine-induced therapeutic T cell-, and not B
589 cell-, dependent antilymphoma immunity. *Blood*.104, 4142-4149. DOI: 10.1182/blood-
590 2009-05-219683.
- 591
592 Radvanyl, F. R., Bon, C., 1982. Catalytic activity and reactivity with p-
593 bromophenacylbromide of the phospholipase subunit of crotoxin. Influence of dimerization
594 and association with the noncatalytic subunit. *J. Biol. Chem.* 257, 12616-12623.
- 595
596 Rodrigues, R.S., Izidoro, L.F., Oliveira, R.J, Sampaio, S.V., Soares, A.M., Rodrigues, V.M.,
597 2009. Snake venom phospholipases A2: a new class of antitumor agents. *Prot. Pept.*
598 *Lett.*16, 894-898.
- 599
600 Rübssamen, K., Breithaupt, H. B, Habermann, E., 1971. Biochemistry and pharmacology of
601 the crotoxin complex I. Subfractionation and recombination of the crotoxin complex.
602 *Naunyn Schmiedebergs Arch Pharmakol.* 270, 274-288.
- 603
604 Rudd, C.J., Viskatis, L.J., Vidal, J.C., Etcheverry, M.A., 1994. In vitro comparison of
605 cytotoxic effects of crotoxin against three human tumors and a normal human epidermal
606 keratinocyte cell line. *Invest New Drugs.* 12,183-184.
- 607
608 Sampaio, S. C., Hyslop, S., Fontes, M.R., Franceschi, J.P., Zambelli, V.O., Magro, A.J.,
609 Brigatte, P., Gutierrez, V.P., Cury, Y., 2010. Crotoxin: novel activities for a classic beta-
610 neurotoxin. *Toxicon.* 55, 1045-1060. DOI: 10.1016/j.toxicon.2010.01.011.
- 611
612 Shevchenko, A., Wilm, M., Vorm, O., Mann, M., 1996. Mass Spectrometric Sequencing of
613 Proteins from Silver-Stained Polyacrylamide Gels. *Anal. Chem.* 68, 850-858. DOI:
614 10.1021/ac950914h.
- 615
616 Siddiqui, M.S., François, M., Fenech, M.F., Leifert, W.R., 2015. Persistent γ H2AX: A
617 promising molecular marker of DNA damage and aging. *Mutat Res Rev.* 766, 1-19. DOI:
618 10.1016/j.mrrev.2015.07.001.
- 619
620 Silva, V.A., Rosa, M., Tansini, A., Silva-Oliveira, R., Martinho, O., Lima, J.P, Pianowski,
621 L.F., Reis, R.M., 2018. In vitro screening of cytotoxic activity of euphol from *Euphorbia*
622 *tirucalli* on a large panel of human cancer-derived cell lines. *Exper. and Ther. Med.* 16,
623 557-566. DOI: 10.3892/etm.2018.6244.
- 624
625 Silva-Oliveira, R.J., Silva, V.A.O., Martinho, O., Cruvinel-Carlioni, A., Melendez, M.E.,
626 Rosa, M.N., de Paula, F.E., Viana, L.S., Carvalho, A.L., Reis, R.M., 2016. Cytotoxicity of
627 allitinib, an irreversible anti-EGFR agent, in a large panel of human cancer-derived cell
628 lines: KRAS mutation status as a predictive biomarker. *Cellular Oncology.* 39, 253-263.
629 DOI: 10.1007/s13402-016-0270-z.
- 630
631 Soares, A.M., Giglio, J.R., 2003. Chemical modifications of phospholipases A2 from snake
632 venoms: Effects on catalytic and pharmacological properties. *Toxicon,* 42, 855-868.
633 DOI:10.1016/j.toxicon.2003.11.004.

634

635

636 Sobrinho, J.C, Simões-Silva, R., Holanda, R., Alfonso, J., Gomez, A.F., Zanchi, F.B.,
637 Moreira-Dill, L.S., Grabner, A.N., Zuliani, J.P., Calderon, L.A., Soares, A.M., 2016.
638 Antitumoral Potential of Snake Venom Phospholipases A2 and Synthetic Peptides. *Curr.*
639 *Pharm. Biotechnol.* 17, 1201-1212. DOI: 10.2174/1389201017666160808154250.

640

641 Suffness M., Pezzuto J.M., 1990. Assays related to cancer drug discovery. In:
642 Hostettmann, K. (Ed.), *Methods in Plant Biochemistry: Assays for Bioactivity*. Academic
643 Press, London, pp.71–133.

644

645 Talib, W. H., 2010. Antiproliferative Activity of Plant Extracts Used Against Cancer in
646 Traditional Medicine. *Sci. Pharm.* 78, 33–45. DOI:10.3797/scipharm.0912-11.

647

648 Teixeira, T.L., Oliveira Silva, V.A., da Cunha, D.B., Poletini, F.L., Thomaz, C.D., Pianca,
649 A.A., Zambom, F.L., Mazzi, D.P.S.L., Reis, R.M., Mazzi, M.V., 2016. Isolation,
650 characterization and screening of the in vitro cytotoxic activity of a novel L-amino acid
651 oxidase (LAAOcdt) from *Crotalus durissus terrificus* venom on human cancer cell lines.
652 *Toxicon.* 119, 203-217, DOI: 10.1016/j.toxicon.2016.06.009.

653

654 Trendowski, M., 2015. Recent Advances in the Development of Antineoplastic Agents
655 Derived from Natural Products. *Drugs*, 75, 1993–2016. DOI: 10.1007/s40265-015-0489-4.

656

657 Voutsadakis, I. A., 2011. Molecular predictors of gemcitabine response in pancreatic
658 cancer. *World journal of gastrointestinal oncology.* 3, 153-164. DOI:
659 10.4251/wjgo.v3.i11.153.

660

661 Wang, J.H., Xie, Y., Wu, J.C., Han, R., Reid, P.F., Qin, Z.H., He, J.K., 2012. Crotoxin
662 enhances the antitumor activity of gefinitib (Iressa) in SK-MES-1 human lung squamous
663 carcinoma cells. *Oncol Rep.* 27,1341-1347. DOI:10.3892/or.2012.1677.

664

665 Wiedmann, M.W., Mossner, J., 2013. New and emerging combination therapies for
666 esophageal cancer. *Cancer management and research.* 5,133-146. Wiedmann, M., &
667 Mössner. (2013). DOI:10.2147/cmar.s32199.

668

669 Yan, C.H., Yang, Y.P., Qin, Z.H., Gu, Z.L., Reid, P., Liang, Z.Q., 2007. Autophagy is
670 involved in cytotoxic effects of crotoxin in human breast cancer cell line MCF-7 cells. *Acta*
671 *Pharmacol.* 28, 540-548. DOI: 10.1111/j.1745-7254.2007.00530.x.

672

673 Ye, B., Xie, Y., Qin, Z.H., Wu, J.C., Han, R., He, J.K., 2011. Anti-tumor activity of CTX in
674 human lung adenocarcinoma cell line A549. *Acta Pharmacol Sin.* 32, 1397-1401. DOI:
675 10.1038/aps.2011.116.

676

677

678

679

680

681 **Figure legends**

682 **Figure 1. Purification and isolation of Crotoxin (CTX).** (A) Ion exchange chromatography
683 of the crude venom of *Crotalus durissus terrificus* on DEAE-c column, which had been
684 previously equilibrated in 0.05 M Tris-HCl, pH 7.5, and eluted in increasing gradient of NaCl
685 (0.1 M) in 0.05 M Tris-HCl, pH 7.5. Fractions of 2 mL were collected and analyzed in a
686 spectrophotometer ($\lambda_{280\text{nm}}$). (B) Heparin-Sepharose FF (HiTrap, heparin (HP), 5 mL) column
687 of the F4 CTX (50 mg) previously equilibrated with 0.01 M sodium phosphate, pH 7.0 and
688 eluted in linear gradient of NaCl (0–1.5 M) at a flow rate of 2.5 mL/ min. Fractions of 3 mL
689 were collected and analyzed in a spectrophotometer ($\lambda_{280\text{nm}}$). (C) SDS-PAGE using a 13%
690 acrylamide-bisacrylamide (w/v) gel in Tris-glycine buffer, pH 8.3. Lane 1: molecular weight
691 markers; lane 2: crude venom (CV) (10 μg); and Lane 3: CTX (10 μg). (D) Mass spectrometry
692 of CTX. Five micrograms of isolated CTX were reduced in 10 mM DTT, alkylated in 50 mM
693 iodoacetamide, and digested with 20 ng/ μL of trypsin. Protein identification was performed in
694 a mass spectrometer coupled to an HPLC using a C18 nanocolumn. The resulting spectra
695 were analyzed using Mascot (Matrix 5 Science) in the NCBI nr protein databases, with
696 carbamidomethylation as the fixed modification. Similar peptide sequences were identified
697 using BLAST. Peptide fragments are observed in b ions (N-terminus), and y ions (C-
698 terminus). a*, b*, and y* represent ion fragments of RKNQ that have lost ammonia (-17 Da). b°
699 represent ion fragments of STED that have lost water (-18 Da).

700

701 **Figure 2. Effect of crotoxin (CTX) on cell viability of normal and human cancer-derived**
702 **cell lines.** Viability of tumor cells was determined by the MTS assay after incubation with
703 different concentrations of crotoxin (0.5–30 $\mu\text{g}/\text{mL}$) for 72 h. (A and B) Esophageal cancer

704 cells (Kyse 270 and Kyse 30). (C-E) Glioma cells (GAMG, HCB 151 and U373). (F and G)
705 Pancreatic cancer cells (PSN-1 and PANC-1). (H-I) Cervical cancer cells (HeLa and SiHa). (J-
706 K) Normal human keratinocytes (HaCaT) and mouse fibroblasts (3T3) respectively. Results
707 from three replicates are reported as the mean percentage of viable cells \pm SD compared to
708 control (DMSO - considered as 100% viability). The results of three replicates were expressed
709 as the mean percentage \pm SD of viable cells relatively to the control (considered as 100%
710 viability). The differences between the means and the significance of the treatments were
711 analyzed with GraphPad Prism (Version 6.01) using Student's t-test. * $P < 0.05$, ** $P < 0.01$,
712 *** $P < 0.001$.

713

714 **Figure 3. Effect of crotoxin (CTX) on cell cycle distribution.** Representative cell cycle
715 analysis by flow cytometry of (A) HCB151 and (C) SiHa cells, in absence (Control - 1%
716 DMSO) or presence of FI CTX (HCB 151, $IC_{50} = 4.1 \mu\text{g/mL}$, SiHa, $IC_{50} = 30 \mu\text{g/mL}$), after 24
717 h. Summary of percentage of cells in each phase of the cell cycle are indicated by bars as the
718 mean \pm SD and differences with $p < 0.005$ in the Student's t-test (**). *n.s.* means non-
719 significant. The X-axis represents the channel number (relative DNA content/cell). The Y-axis
720 represents the number of cells/channel.

721

722 **Figure 4. Effect of crotoxin (CTX) on cell death mechanisms.** After 24 h treatment with
723 crotoxin, (A) HCB151 and (C) SiHa cells were fixed, stained with annexin V / PI, and analyzed
724 by flow cytometry using FACScan. The data represent three independent experiments. Non-
725 treated CTR: DMSO (1%) and crotoxin-treated cells (HCB151, $IC_{50} = 4.1 \mu\text{g/mL}$; SiHa, $IC_{50} =$
726 $30 \mu\text{g/mL}$). (B-D) Bars represent the percentage of apoptotic cells as the mean \pm SD and
727 differences with $p < 0.005$ in the Student's t-test (**). *n.s.* non-significant.

728

729

730 **Figure 5. Effect of crotoxin (CTX) on protein profile of human cancer-derived cell lines.**

731 (A) Drug-sensitive (HCB151 and PANC-1) and drug-resistant (SiHa) cells were incubated with
732 crotoxin at the IC_{50} of 4.1 $\mu\text{g}/\mu\text{L}$, 0.5 $\mu\text{g}/\mu\text{L}$ and 30 $\mu\text{g}/\mu\text{L}$ respectively for 24 h. DMSO (1%)
733 was used as negative control. The cell extracts were subjected to Western blotting to analyze
734 the protein expression levels. B-tubulin was used as internal control. (B) Densitometry with
735 levels of protein activity. Proteins were quantified by the ImageJ program. The asterisks (**)
736 indicate statistical significance ($p < 0.005$) between control and experimental group in the
737 Student's t test. *n.s.* non-significant.

738

739 **Tables**

740

741 **Table 1** The CTX, temozolomide, gemcitabine, paclitaxel, and cisplatin half-maximal inhibitory
742 concentration (IC_{50}) against the human cancer-derived cell lines.

743

744

Table 1 The F1 CTX, temozolomide, gemcitabine, paclitaxel, and cisplatin half-maximal inhibitory concentration (IC₅₀) against human cancer-derived cell lines.

Cell line	F1 CTX Mean IC ₅₀ ±S.D (μ g/mL)	Temozolomide Mean IC ₅₀ ± S.D (μ g/mL)	Gemcitabine Mean IC ₅₀ ± S.D (μ g/mL)	Paclitaxel Mean IC ₅₀ ± S.D (μ g/mL)	Cisplatin Mean IC ₅₀ ± S.D (μ g/mL)	Origin	Organism	Tissue	Culture conditions
GAMG	< 0.5	18.8± 2.0	ND	ND	ND	Glioblastoma	Human	Brain	DMEM + 10% FBS + 1% P/S
U373	30.1±1.5	105.7± 1.5	ND	ND	ND	Glioblastoma astrocytoma	Human	Brain	DMEM + 10% FBS + 1% P/S
HCB151	4.1±3.8	17.5±0.5	ND	ND	ND	Primary glioma	Human	Brain	DMEM + 10% FBS + 1% P/S
PANC-1	< 0.5	ND	8.8±2.6	ND	ND	Pancreatic cancer	Human	Pancreas	DMEM + 10% FBS + 1% P/S
PSN-1	0.69±0.08	ND	1.4±0.02	ND	ND	Pancreatic cancer	Human	Pancreas	DMEM + 10% FBS + 1% P/S
KYSE30	0.9±1.7	ND	ND	0.005± 0.003	ND	Squamous cell carcinoma	Human	esophagus	RPMI 1640 + 10% FBS + 1% P/S
KYSE270	8.7±1.4	ND	ND	0.006±0.002	ND	Squamous cell carcinoma	Human	esophagus	RPMI 1640 + 10% FBS + 1% P/S
HeLa	2.4±1.1	ND	ND	ND	6.3±1.8	Cervix carcinoma	Human	Cervix	DMEM + 10% FBS + 1% P/S
SiHa	>30	ND	ND	ND	14.9±3.6	Squamous Cell Carcinoma	Human	Cervix	DMEM + 10% FBS + 1% P/S
NHI/3T3	>30	ND	ND	ND	ND	Fibroblast	Mouse	Embryo	DMEM + 10% FBS + 1% P/S
HaCat	>30	ND	ND	ND	ND	Normal Keratinocytes	Human	Skin	DMEM + 10% FBS + 1% P/S

FBS. Fetal Bovine Serum; P/S Penicillin/Streptomycin solution; ND. Not done. All the assays were done in triplicate and repeated at least three times.

Highlights

Crotoxin demonstrated cytotoxic effect on different tumor cell lines.

The molecule had a heterogeneous cytotoxic effect on the different tumor lines.

The glioma and pancreatic cancer cells showed a higher sensitivity.

Cervical and esophagus cancer cell lines presented higher resistance.